



1 **Extreme Heat and Wildfire Emissions Enhance Volatile Organic**
2 **Compounds: Insights on Future Climate**

3 Christian Mark Salvador^{1,#}, Jeffrey Wood², Emma Cochran², Hunter Seubert², Bella Kamplain²,
4 Sam Overby², Kevin Birdwell¹, Lianhong Gu¹, Melanie Mayes^{1,#}

5 ¹*Environmental Sciences Division, Oak Ridge National Laboratory, Oak Ridge, TN, USA*

6 ²*School of Natural Resources, University of Missouri, Columbia, MO, USA*

7

8 *Correspondence to:* Christian Mark Salvador (salvadorcg@ornl.gov) and Melanie Mayes (mayesma@ornl.gov)

9

10

11 **Abstract.** Climate extremes are projected to cause unprecedented deviations in the emission and transformation of
12 volatile organic compounds (VOCs), which trigger feedback mechanisms that will impact the atmospheric oxidation
13 and formation of aerosols and clouds. However, the response of VOCs to future conditions such as extreme heat and
14 wildfire events is still uncertain. This study explored the modification of the mixing ratio and distribution of several
15 anthropogenic and biogenic VOCs in a temperate oak–hickory–juniper forest as a response to increased temperature
16 and transported biomass burning plumes. A chemical ionization mass spectrometer was deployed on a tower at a
17 height of 32 m in rural central Missouri, United States, for the continuous and in situ measurement of VOCs from
18 June to August of 2023. The maximum observed temperature in the region was 38°C, and during multiple episodes
19 the temperature remained above 32°C for several hours. Biogenic VOCs such as isoprene and monoterpene followed
20 closely the temperature daily profile but at varying rates, whereas anthropogenic VOCs were insensitive to elevated
21 temperature. During the measurement period, wildfire emissions were transported to the site and substantially
22 increased the mixing ratios of acetonitrile and benzene, which are produced from burning of biomass. An in-depth
23 analysis of the mass spectra revealed more than 250 minor compounds, such as formamide and methylglyoxal. The
24 overall volatility, O:C, and H:C ratios of the extended list of VOCs responded to the changes in extreme heat and the
25 presence of combustion plumes. Multivariate analysis also clustered the compounds into five factors, which
26 highlighted the sources of the unaccounted-for VOCs. Overall, results here underscore the imminent effect of extreme
27 heat and wildfire on VOC variability, which is important in understanding future interactions between climate and
28 atmospheric chemistry.

29

30 *Copyright statement:* This manuscript has been authored by UT-Battelle, LLC, under contract no. DE-AC05-
31 00OR22725 with the US Department of Energy (DOE). The US government retains and the publisher, by accepting
32 the article for publication, acknowledges that the US government retains a nonexclusive, paid-up, irrevocable,
33 worldwide license to publish or reproduce the published form of this manuscript, or allow others to do so, for US
34 government purposes. DOE will provide public access to these results of federally sponsored research in accordance
35 with the DOE Public Access Plan (<http://energy.gov/downloads/doe-publicaccess-plan>).

36

37



38 1. Introduction

39 Future global climate, with continuing greenhouse gas emissions such as CO₂ from the burning of fossil fuels, is
40 expected to have warmer temperatures that impact critical atmospheric processes. Global averaged surface air
41 temperature is projected to exceed 1.5°C relative to 1850–1900 by the year 2030, regardless of the emission scenarios.
42 Looking further to the future, 2081 to 2100 will experience an additional increase of 0.2°C–1.0°C and 2.4°C–4.8°C
43 in low and high emissions scenarios, respectively (Lee et al., 2021). The heating of the atmosphere in the future will
44 have severe effects on several atmospheric components and processes. For instance, a series of models have shown
45 that warming due to greenhouse gas emissions will induce an increase in the global annual average mixing ratios of
46 particles with less than 2.5 µm diameter (PM_{2.5}) (Park et al., 2020), which will have grave implications for air quality,
47 climate, and human cardiovascular health. By 2050, the elevated temperature is projected to increase PM_{2.5} by
48 2–3 µg m⁻³ in the summer of the eastern United States as a consequence of faster oxidation rates and elevated
49 production of organic aerosols (Shen et al., 2017). There is thus an urgent need to elucidate the impact of extreme heat
50 on atmospheric processes, including the emission and transformation of organic compounds, to understand future
51 aerosol-generating scenarios.

52

53 One potential effect of overall atmospheric warming is the alteration wildfire events' frequency around the globe
54 (Varga et al., 2022; Sarris et al., 2014; Ruffault et al., 2018). At elevated temperatures, evaporation of soil moisture
55 and generation of more fuel from drying vegetation are more pronounced, thus inducing more wildfire events. Beyond
56 the CO₂ emissions, wildfires generate thousands of carbonaceous compounds that impact global climate air quality
57 and human health (Schneider et al., 2024a). With the elevated prevalence of wildfires with prolonged duration,
58 extreme wildfire events are expected to impact the future mixing ratio and distribution of atmospheric chemical
59 compounds that influence relevant processes such as aerosol and cloud formation. For instance, global-scale airborne
60 measurements showed increased tropospheric ozone in air masses influenced by biomass-burning (BB) events
61 (Bourgeois et al., 2021). Long-term analysis of wildfire events in Western Canada (2001–2019) also indicated an
62 increase in the average ozone mixing ratio (~2 ppb), particularly during events with high mixing ratios of atmospheric
63 aerosols from combustion (Schneider et al., 2024b). Ozone enhancement will lead to elevated atmospheric oxidation
64 capacity that can initiate more secondary pollutant formation.

65

66 Among the chemical components of the atmosphere, volatile organic compounds (VOCs) are expected to respond to
67 extreme heat and wildfire emissions. VOCs, particularly the unsaturated compounds, interact with oxidants such as
68 hydroxyl (OH) and nitrate (NO₃) radicals, which subsequently create ozone and oxidized molecules (Hakola et al.,
69 2012; Ramasamy et al., 2016; Spirig et al., 2004; Vermeuel et al., 2023). Further reaction products such as highly
70 oxidized molecules also participate in the formation of particles that subsequently act as cloud condensation nuclei
71 (Chen et al., 2022; Hallquist et al., 2009). The emission and transformation of VOCs highly depend on environmental
72 parameters such as temperature, relative humidity, and solar radiation, but the degree of changes under future climate
73 is still uncertain (i.e., suppression or enhancement) (Daussy and Staudt, 2020). For instance, a global estimate of
74 isoprene emissions with future temperature and land-cover drivers was 889 Tg yr⁻¹, substantially higher compared to



75 that expected using current climatological and land-cover conditions (522 Tg yr^{-1}) (Wiedinmyer et al., 2006).
76 However, CO_2 , which is expected to rise in future climate, can substantially decrease the emission of isoprene from
77 vegetation (Lantz et al., 2019a). On the other hand, empirical results and modeling efforts suggest that future elevated
78 temperatures could suppress the impact of CO_2 on isoprene emissions, thus increasing the uncertainty of future
79 climate's influence on the emission of isoprene (Lantz et al., 2019b; Sahu et al., 2023). The complexity of the
80 interaction between abiotic factors of the future and the emission of VOCs should be fully understood to better predict
81 future air quality and climate scenarios.

82

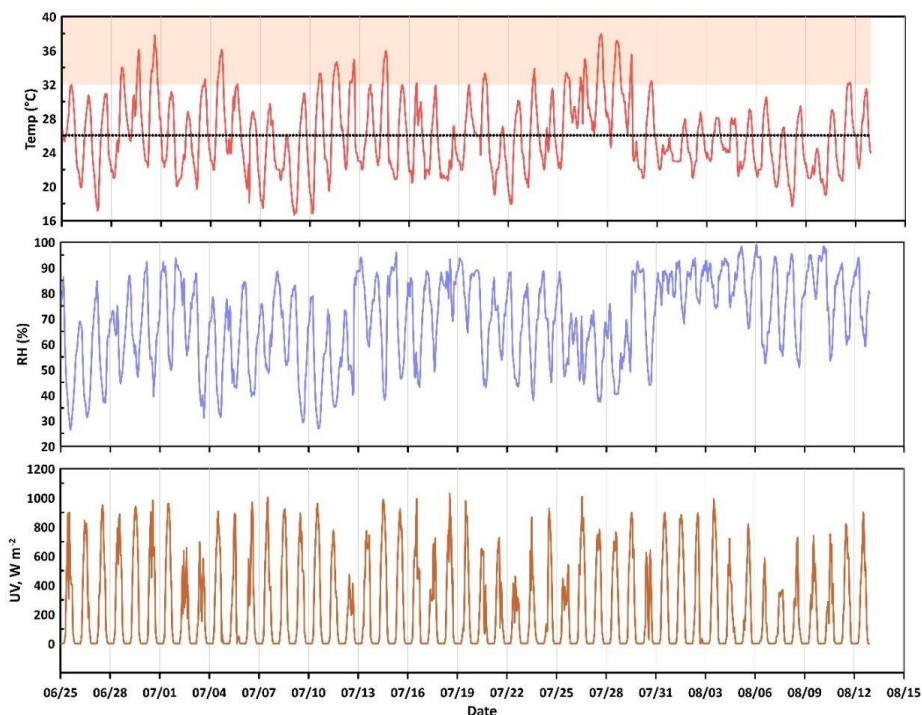
83 In this work, we conducted a field campaign in the summer of 2023 to quantify the variability of VOCs over a
84 temperate oak–hickory–juniper (*Quercus–Carya–Juniperus*) forest in the Ozark Border Region of central Missouri.
85 The primary goal of the campaign was to examine the influence of temperature on VOCs. However, we were also able
86 to incorporate opportunistic analyses of smoke plumes that reached our site because of extreme wildfire activity in
87 Canada. We deployed a high-resolution chemical ionization mass spectrometer to continuously measure VOC
88 concentrations. The mass resolution of the technique ($6000 \text{ m}/\Delta\text{m}$) provided an extended list of VOCs, beyond the
89 usual routinely evaluated compounds (e.g., methanol, isoprene, and monoterpene). The Ozark Plateau (Wiedinmyer
90 et al., 2005), and this site in particular, is a known hotspot for biogenic VOC (BVOC) emissions. Given these strong
91 emitters of BVOCs and the evident transport of anthropogenic VOCs (AVOCs) into the forest, the study area proved
92 to be a good test bed for measurement of the overall response of VOCs to abiotic stress in a way that simulates possible
93 future atmospheric conditions. The results presented here provide important information to assess possible future
94 feedback loops of vegetation and atmospheric chemistry to regional- and/or global-scale climate changes.

95



96 **2. Experimental Designs**

97 **2.1 Site Description and Meteorological Data**



98

99 **Figure 1.** Time series profile of (top) temperature, (mid) relative humidity, RH, and (bottom) global solar radiation,
 100 UV, at the temperate mixed deciduous forest in Missouri. The dotted line in the temperature plot is the average value
 101 during the measurement duration, and the shaded filled area denotes the extreme temperature conditions ($>32^{\circ}\text{C}$).

102 Measurements were conducted at the Missouri Ozark AmeriFlux (MOFLUX) site (latitude 38.7441,
 103 longitude -92.2000) in central Missouri, United States. The MOFLUX site is registered with the AmeriFlux (ID: US-
 104 MOz) and PhenoCam networks (ID: missouriozarks). The campaign was conducted during the summer of 2023,
 105 between June 25 and August 12. The site is situated in the Baskett Wildfire Research and Education Area. The primary
 106 sources of BVOCs were oaks (white and black), sugar maple, shagbark hickory, and eastern red cedar (Geron et al.,
 107 2016). The subtropical/mid-latitude continental characteristics of the area provide a warm and humid overall climate
 108 for the forest. Long-term measurements of meteorological parameters (1981–2010) at a nearby airport
 109 (~ 10 km) indicated that the average temperatures for January and July were -1°C and 25.2°C (National Climatic Data
 110 Center citation). Typical annual precipitation is fairly evenly distributed through the annual cycle and averages
 111 1082 mm. More information regarding the site is provided elsewhere (Gu et al., 2015).

112

113 Figure 1 shows the time series profile of hourly averages of temperature and relative humidity collected from
 114 Columbia Regional Airport (38.817, -92.221), approximately 8.5 km from the MOFLUX site. Global solar radiation
 115 data were measured at a weather site in Ashland, MO (38.722, -92.253), 5.22 km from the MOFLUX tower. The data



116 were accessed using the MesoWest online website (<https://mesowest.utah.edu/>) provided by the Department of
117 Atmospheric Sciences, University of Utah. The average (absolute min-max) temperature, relative humidity (RH),
118 global solar radiation, and wind speed (not shown in the figure), were 26°C (16–38°C), 69.01% (26.43–99.02),
119 228 W m⁻² (0–1028 W m⁻²), and 3.2 m s⁻² (0–11.27 m s⁻²) during the time of VOC measurements. The diurnal profiles
120 of the meteorological conditions are provided in the supplement. During the weeks of July 4 and July 11, 64 and 100%
121 cumulative percent area reported abnormally dry conditions (D0, US Drought Monitor Category). Drought data were
122 accessed from the U.S. Drought Monitor (<https://droughtmonitor.unl.edu/>). Drought is a critical event at MOFLUX,
123 as such environmental stress induced the highest ecosystem isoprene emission ever recorded for a temperate forest in
124 2011 (53.3 mg m⁻² h⁻¹) (Potosnak et al., 2014). Smoke mixing ratios (in mg m⁻³) were estimated from the High-
125 Resolution Rapid Refresh (HRRR) 3 km weather model for Missouri at 6 hour intervals for the duration of the VOC
126 data measurement period. Values ranged from 0 to 10 mg m⁻³ during 80% of the measurement dates (overall average
127 was 7.33 mg m⁻³) but reached a maximum of 175 mg m⁻³ on July 16 in association with drift from large Canadian
128 wildfires.

129 2.2 VOC Measurement and Identification

130 VOCs were measured using a proton transfer reaction time of flight mass spectrometer (PTR-ToF-MS 6000 X2)
131 (Ionicon Analytik Ges.m.b.H., Innsbruck, Austria). A detailed description of the general mechanism of the PTR-ToF-
132 MS can be found elsewhere (Yuan et al., 2017). Briefly, hydronium ions are utilized to charge the VOCs through a
133 non-dissociative proton transfer in the reaction chamber of the instrument. This technique can identify a wide range
134 of compounds (e.g., carboxylic acids, carbonyls, and aromatic hydrocarbons) if the target compound has a proton
135 affinity higher than water (691 kJ/mol). The protonation occurs as follows:

136



138

139 The PTR-ToF-MS was calibrated regularly using a 110 ppb mixture of gases (isoprene, limonene, benzene, toluene,
140 ethylbenzene, dichlorobenzene, trichlorobenzene, and trimethylbenzene, Restek Corp). The linear calibration curve
141 consisted of eleven data points, with mixing ratios ranging between 1.89 and 50.9 ppb. The same compounds were
142 used to calculate the mixing ratio of other compounds using the transmission efficiency and first-order kinetic reaction.
143 The PTR-ToF-MS was operated with 2.6 mbar and 80°C drift tube pressure and temperature, with an E/N value of
144 ~119 Townsend. The mass range was set up to 500 m/z with a time resolution of 100 ms. The single spectrum time
145 was set to calculate the fluxes of the VOC, the results of which will be reported in subsequent works. One of the
146 limitations of the PTR-ToF-MS technique is that it cannot distinguish isomers (e.g., α -pinene, β -pinene, and limonene)
147 because of their identical exact mass (Blake et al., 2009). Instrument blank was measured hourly using a series of
148 switching valves and Ultra Zero grade air (Airgas).

149



150 Ambient air was sampled from the MOFLUX tower. The air was drawn at the top of the tower using a ½ in. OD PFA
151 tube (McMaster-Carr) and a GAST compressor/vacuum pump with a mass flow controller (Alicat Scientific, Inc) set
152 at 20 L min⁻¹.

153

154 High-resolution peak analysis, chemical formula identification, and data quantification were performed using the
155 IONICON data Analyzer (IDA). IDA identified more than 1000 ions, which were subsequently reduced to 275 peaks
156 with more than 5 parts per trillion (ppt) mixing ratios above the average blank data. Here, *mixing ratio* is defined as
157 the ratio of the moles of target analyte to the moles of all of atmospheric gases (i.e., N₂ and O₂). This can be expressed
158 as the following equation:

159

$$R_i = \frac{n_i}{n_\Sigma - n_i} \approx \frac{n_i}{n_\Sigma} \quad (2)$$

160 Where R_i is the mixing ratio, n_i is the moles of gas analyte, and n_Σ is the total moles of atmospheric gases. The amount
161 of organic gases in the atmosphere is significantly lower than the total gases. The chemical identification procedure
162 was complemented by an analysis using ChemCalc, which also provided the theoretical masses and degree of
163 saturation (Patiny and Borel, 2013).

164 2.3 Source and Process Signature Analysis of VOCs using Multivariate Analysis

165 Determination of the source signature or emission profile of the VOCs is critical in assessing the dominant
166 anthropogenic and biogenic activities that impact the atmospheric reactivity from VOCs. Here, multivariate analysis
167 was applied to the observed VOC mixing ratios using non-negative matrix factorization (NNMF). Because NNMF
168 requires no uncertainty for the calculation procedure, it has an advantage over positive matrix factorization, which is
169 typically implemented for a mixture of organic compounds in the gas and particle phase (Salvador et al., 2022). NNMF
170 is expressed as

171

$$A_{m \times n} = W_{m \times k} H_{k \times n} + \sigma_{m \times n} \quad (3)$$

172

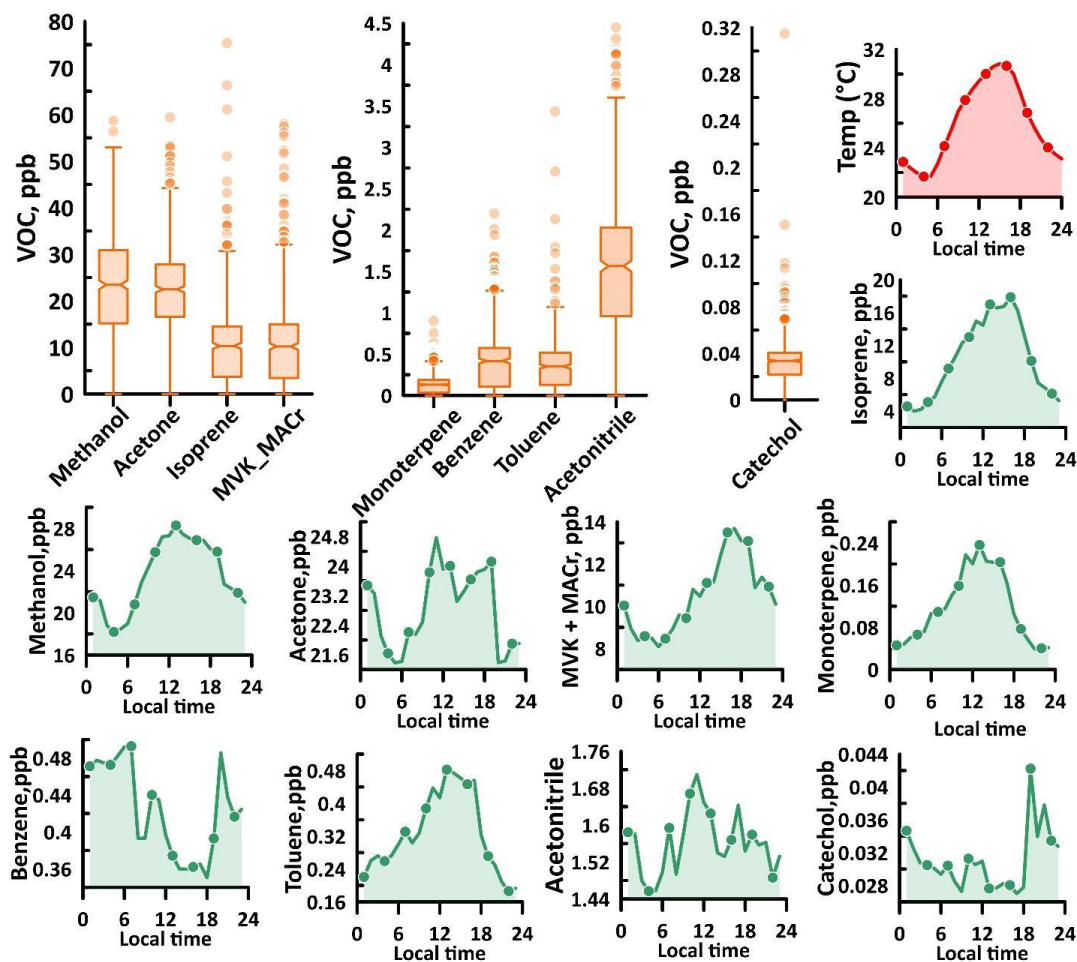
173 where A is the input matrix with dimensions of m and n containing non-negative elements, W and H are species
174 fingerprint and coefficient matrices, k is the lowest rank approximation or the optimal factor, and σ is the residual
175 between the left and right sides of the equation. The VOC mixing ratio data with a matrix of 196×274 dimensions
176 was employed as the input for the NNMF routine program in MATLAB. The NNMF was applied for a 10-factor series
177 with 30 replicates, 1000 iterations, and a multiplicative update algorithm. The five-factor solution was the optimal
178 number used for the analysis based on the calculated root mean square of the residuals and the variability of the major
179 tracers across the factors.

180



181 3. Results and Discussion

182 3.1 General Overview of the Major VOCs



183

184 **Figure 2.** Average mixing ratio in ppb (top left) and diurnal profile of some of the major VOCs at MOFLUX. Time reported here
 185 is the local daylight time. The center lines of the box and whisker plots are the mean mixing ratio. Box edges are quartiles, and
 186 lower (upper) corresponds to 25th (75th). Whiskers represent 1.5 times the interquartile range. Symbols outside the box plot are
 187 outliers. Diurnal profiles have a unit of ppb mixing ratio. MVK and MACr are methyl vinyl ketone and methacrolein. The average
 188 diurnal profile of temperature (top right) is also provided for reference.
 189

190 Several VOCs were detected in the ambient air throughout the three-month measurement period. Figure 2 shows the
 191 average mixing ratio of the dominant VOCs observed in the temperate forest. Among the VOCs, methanol and acetone
 192 recorded the highest mixing ratios. Methanol and acetone are the most abundant nonmethane organic gases in the
 193 troposphere and are emitted by terrestrial plants during growth stages (Bates et al., 2021; Hu et al., 2013; Wells et al.,
 194 2014). Mean mixing ratios of the methanol and acetone were 23 ppb, consistent with a prior study done in MOFLUX,
 195 in which half-hour averages of methanol ranged between 1.9 and 26 ppb (Seco et al., 2015). Here, the maximum



196 hourly average mixing ratio of methanol reached as high as 59 ppb, which occurred at 6:00 pm on the 30th of June.
197 Methanol also showed a diurnal profile with a daily peak at noon, which was an indication of a photochemical source.
198 Besides the terrestrial emissions of methanol, the secondary production of methanol from organic peroxyradicals (e.g.,
199 CH₃O₂) contributes substantially to the methanol budget (Bates et al., 2021).

200

201 Also shown in Figure 2 are the average mixing ratios of isoprene and its primary oxidation products, methyl vinyl
202 ketone and methacrolein (MVK+MACr). Isoprene is the most dominant BVOC, contributing around 50% to the total
203 global budget (Guenther et al., 2012). Isoprene substantially influences the surface ozone concentration and secondary
204 organic aerosol formation, which is attributed to isoprene's reactivity to ozone, OH, and nitrate (NO₃) radicals
205 (Wennberg et al., 2018). Besides the photochemical oxidation of isoprene, MVK and MACr have other sources, such
206 as BB and gasoline vehicular emissions (Ling et al., 2019). Isoprene also generates MVK during nighttime through
207 the dominant β-RO₂ isomer formation pathway (Ng et al., 2017). Isoprene's emission rate at MOFLUX was previously
208 reported as one of the highest for canopy-scale emissions (53.3 mg m⁻² h⁻¹) (Potosnak et al., 2014). This was evident
209 in our measurement, where the average mixing ratio of isoprene during the intensive observation period was 10.32
210 ppb, and MVK + MACr had a similar mean mixing ratio. The isoprene mixing ratio reached as much as 75 ppb, which
211 occurred at 1:00 pm on July 4. Observed isoprene mixing ratios were substantially elevated compared to other similar
212 temperate forests in the United Kingdom (~8 ppb) (Ferracci et al., 2020), deciduous forest in Michigan, USA (~1.5
213 ppb) (Kanawade et al., 2011), and mixed temperate forest in Canada (~0.01 ppb) (Fuentes and Wang, 1999). For
214 MVK+MACr, prior measurements in similar environments reported mixing ratios below 2.0 ppb (Safronov et al.,
215 2019; Shtabkin et al., 2019; Montzka et al., 1995) highlighting the intense production of MVK+MACr at MOFLUX.
216 Interestingly, the most elevated mixing ratio of MVK+MACr (58 ppb) occurred on a different day (6/28) and later in
217 the night (8:00 pm); this result was attributed to other sources of MVK and MACr. Nevertheless, the MVK showed a
218 similar diurnal profile with isoprene, which suggested that photochemical oxidation of isoprene was the dominant
219 source of MVK+MACr observed in MOFLUX. Also, diurnal profiles, as indicated in Figure 2, showed that
220 MVK+MACr still persisted even with the reduction of the isoprene at nighttime. This was attributed to the longer
221 atmospheric lifetime and lesser reactivity of MVK+MACr.

222

223 Monoterpene, a critical contributor to ozone and secondary aerosol formation (Salvador, 2020; Salvador et al., 2020b),
224 is composed of several organic species such as α-pinene, β-pinene, limonene, δ-carene, ocimene, and sabinene, and
225 its distribution varies significantly based on the vegetation species. At MOFLUX, monoterpenes had an average
226 mixing ratio of less than 0.2 ppb, as shown in Figure 2. Throughout the measurement duration, the maximum mixing
227 ratio of monoterpene was 0.9 ppb. This ambient level is similar to a prior measurement at the MOFLUX site (Seco et
228 al., 2015), as well as observations of monoterpene in other temperate forests in Wisconsin, USA, and Wakayama,
229 Japan (Vermeuel et al., 2023; Ramasamy et al., 2016). Interestingly, the diurnal profile of monoterpene at MOFLUX
230 had a daytime peak, which is not typical compared to other observations of monoterpene with nighttime enhancements
231 (Gentner et al., 2014; Stewart et al., 2021; Salvador et al., 2020a). Regions dominated by emissions of α-pinene, β-
232 pinene, and limonene typically have a nighttime peak, whereas daytime enhancements are observed for areas with



233 sabinene and ocimene (Hakola et al., 2012; Gentner et al., 2014; Jardine et al., 2015; Borsdorf et al., 2023). Either of
234 the latter two VOCs or a combination thereof might be the main monoterpenes impacting the chemical reactivity at
235 MOFLUX leading to aerosol formation in the forest. Particle size distribution analysis (see Figure S2) at our temperate
236 forest indicated no evident particle formation events. Relatively large particles (i.e., particle diameter \approx 50 nm) were
237 observed with no apparent aerosol growth. Prior study also showed less frequent new particle formation events,
238 particularly during the influence of southerly air masses rich in BVOCs (Yu et al., 2014). The most probable reason
239 for the presence of these large particles was the isoprene-rich condition of the temperate forest that impacted the
240 aerosol nucleation, even with enough monoterpene and ozone available for particle formation. Prior plant chamber
241 analysis indicated that the suppression of new particle formation was dependent on the ratio of isoprene carbon to
242 monoterpene carbon (Kiehl-Scharr et al., 2009). The mixing of isoprene and monoterpene also impacts the
243 atmospheric oxidation capacity, in which isoprene scavenges the OH radicals (McFiggans et al., 2019). Recent studies
244 also showed that the mixing of isoprene to monoterpene reduced C₂₀ dimers that drive aerosol formation at mixed
245 biogenic precursor systems (Heinritzi et al., 2020). At MOFLUX, the median ratio of isoprene carbon to monoterpene
246 carbon was 42, which is significantly higher compared to measurements in forests in Alabama (Lee et al., 2016),
247 Michigan (Kanawade et al., 2011), the Amazon (Greenberg et al., 2004), and Finland (Spirig et al., 2004). Ratios
248 above 20 completely limit the formation of aerosols, which is consistent with the observations at MOFLUX.

249

250 Besides biogenic VOCs, several anthropogenic-related VOCs were detected in the temperate forest. The site is about
251 5 km away from a major highway, which possibly contributed to the diversity of VOCs at MOFLUX. During the
252 measurement period, benzene, a VOC usually emitted from automobile exhausts, had a mean mixing ratio of
253 0.42 ppb, with a maximum of 2.2 ppb. Benzene had mixing ratio peaks consistent with the traffic (8:00 and 20:00)
254 with no evident noontime peak. Similar to biogenic precursors, benzene can also initiate particle formation events,
255 particularly at low NO_x conditions (Ng et al., 2007; Li et al., 2016). The mixing of the biogenic (e.g., isoprene and
256 monoterpene) and anthropogenic VOCs (e.g., benzene) at MOFLUX can introduce unaccounted-for molecular
257 interactions (Voliotis et al., 2021) that can influence the formation of aerosols in the forest. Toluene, another important
258 aromatic VOC from urban emissions, was also observed at a significant amount at the site (\approx 0.3 ppb, mean) with a
259 max mixing ratio of 3.4 ppb. The noontime peak of the toluene daily cycle was unexpected because it usually tracks
260 with traffic conditions. Interference of para-Cymene fragmentation in the drift tube of the PTR-ToF-MS at mass 93
261 (Ambrose et al., 2010) might have impacted the observed concentrations at MOFLUX.

262

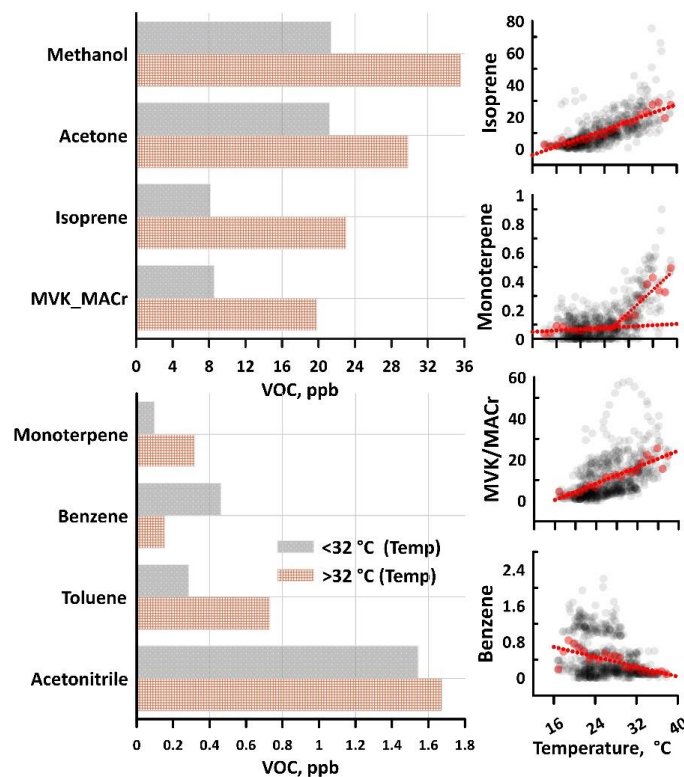
263 Typical gas phase BB tracers were also observed in substantial amounts in MOFLUX. Acetonitrile, one of the
264 prominent BB markers (Huangfu et al., 2021), had mean and maximum mixing ratios of 1.56 ppb and 4.45 ppb,
265 respectively. Such values are beyond the mixing ratio range (0.047 to 1.08 ppb) of acetonitrile recorded in Asian, US,
266 and European regions (Huangfu et al., 2021), highlighting the severe impact of BB in the atmospheric VOC
267 distribution and reactivity of MOFLUX. Acetonitrile did not follow a typical daily cycle, which is consistent with the
268 sporadic nature of the emissions and transport. Another prominent BB marker measured at the site was catechol, an
269 aromatic compound directly emitted from combustion processes. At MOFLUX, catechol had a mean level of 30 ppt



270 but increased significantly to 300 ppt on some days. Catechol had a minor peak during the daytime, which can be
 271 attributed to the photochemical processing of phenol (Finewax et al., 2018), another aromatic VOC emitted during
 272 BB events.

273 3.2 Impact of Extreme Temperatures on VOCs

274 During some parts of the measurement period, mid-Missouri experienced extreme temperature conditions
 275 that impacted the physiochemical processes of the vegetation and the atmosphere. During the measurement period,
 276 the average temperature was 26°C, and the highest hourly value was 38°C. The average temperature was close to the
 277 reported long-term mean temperature in the region; however, the period of measurement exhibited extreme
 278 temperatures that impacted VOC emissions. Diurnal profile temperature showed a daily peak occurring at 15:00,
 279 which typically had a 29.9°C mean temperature. The extreme temperature, defined by an hourly mean temperature
 280 over 32 °C, was based on the projected climate scenarios that temperature will increase by 2–4°C by 2100 (Collins et
 281 al., 2013). The extreme temperature occurred for more than 100 hours (see Figure S1 for histogram). The strong impact
 282 of the elevated temperature in the region ultimately altered the vegetation’s physiological functions.



283

284 **Figure 3.** (Left) Comparison of VOC mixing ratios for temperatures below and above 32°C. Catechol, not shown here, showed no
 285 evident difference between the two conditions (~30 ppt). (Right) The correlation analysis of temperature with biogenic VOCs and
 286 benzene mixing ratios (in ppb). Correlation analysis of other major VOCs is provided in the supplement. Black symbols are hourly
 287 data, whereas the red lines indicate the best-fit line of the binned mixing ratio of VOCs according to 1.0°C of temperature. Note
 288 that monoterpene has two best fit lines that showcase the response of monoterpene at different temperature regimes.



289 BVOCs have different responses to elevated temperatures. Isoprene, for instance, was observed to follow ($r = 0.95$)
290 closely the temperature profile in the region (Figure 3). Linear regression of the temperature and isoprene indicated
291 that an increase of 1.0°C results in 1.32 ppb of isoprene. Moreover, the isoprene mean mixing ratio at elevated
292 temperatures was 23 ppb, which was thrice compared to conditions below 32°C . Monoterpene at MOFLUX also
293 showcased a complex response to temperature. Below 27.8°C , the monoterpene was insensitive to the temperature
294 ($0.0023 \text{ ppb}/^{\circ}\text{C}$, $r = 0.42$) but showed a direct response at enhanced temperatures ($0.0392 \text{ ppb}/^{\circ}\text{C}$, $r = 0.92$). The ten-
295 fold increase in the dependence of monoterpenes on extreme temperature had several implications for the distribution
296 and chemical reactivity in the forest. The non-linear pattern of monoterpene was consistent with the profile of ocimene
297 and sabinene when exposed to a temperature range between 28 and 40°C (Jardine et al., 2017), supporting the initial
298 assessment of the possible dominant monoterpenes at MOFLUX. However, we are not discounting the potential
299 contribution of monoterpenes (e.g., limonene) that are insensitive to changes in temperature. Moreover, the non-linear
300 response of monoterpene to temperature also impacted the aerosol formation events at MOFLUX. A normal
301 distribution of the average ratio of isoprene carbon to monoterpene carbon binned per 1.0°C was calculated (see Figure
302 S4). Even though the values exceeded ratios in which aerosol formation is suppressed, it was interesting that an
303 optimum temperature existed at which the distribution of BVOCs would result in a maximum inhibition of aerosol
304 formation.

305

306 MVK and MACr produced from the oxidation of isoprene showed a strong association with temperature ($1.0 \text{ ppb}/^{\circ}\text{C}$,
307 $r = 0.95$). MVK and MACr reached a 20 ppb average mixing ratio during extreme temperature conditions. This result
308 is twice the ratio at low temperature in the forest, similar to the observed pattern with isoprene. This was consistent
309 with a previous chamber study, which showed that the observed yields of MVK+MACr increased to 17–22% at
310 enhanced temperatures (70°C), compared to 9–11% at 30°C . Several possible causes can be attributed to such
311 observations. First, the higher mixing ratio of precursor isoprene yielded more MVK+MACr in the atmosphere.
312 Moreover, several of the reaction mechanisms during the oxidation of isoprene are temperature dependent (e.g., 1,6-
313 and 1,5-H shift isomerization reactions of isoprene), which further augmented the formation of the first-generation
314 products of isoprene (Navarro et al., 2013).

315

316 Anthropogenic tracers generated from transportation and BB showed little to no dependence on temperature. For
317 benzene ($-0.027 \text{ ppb}/^{\circ}\text{C}$) and xylene ($-0.0069 \text{ ppb}/^{\circ}\text{C}$), an indirect relationship with temperature was recorded. Such
318 results were attributed to the reduction of the height of the primary boundary layer at nighttime, which enhanced the
319 mixing ratio of such AVOCs. With colder temperatures during nighttime, a negative correlation between temperature
320 and AVOCs was expected. Remarkably, the toluene mixing ratio (0.73 ppb) doubled at higher temperatures, unlike
321 the benzene and xylene. This result further affirmed the initial claim that the compound occurring at mass 93 stemmed
322 from the fragmentation of a monoterpene with direct association with temperature. Combustion markers such as
323 acetonitrile ($r = 0.53$) and catechol ($r = 0.017$) also did not follow the trend of temperature, which is consistent with
324 the infrequent emissions of BB plumes.

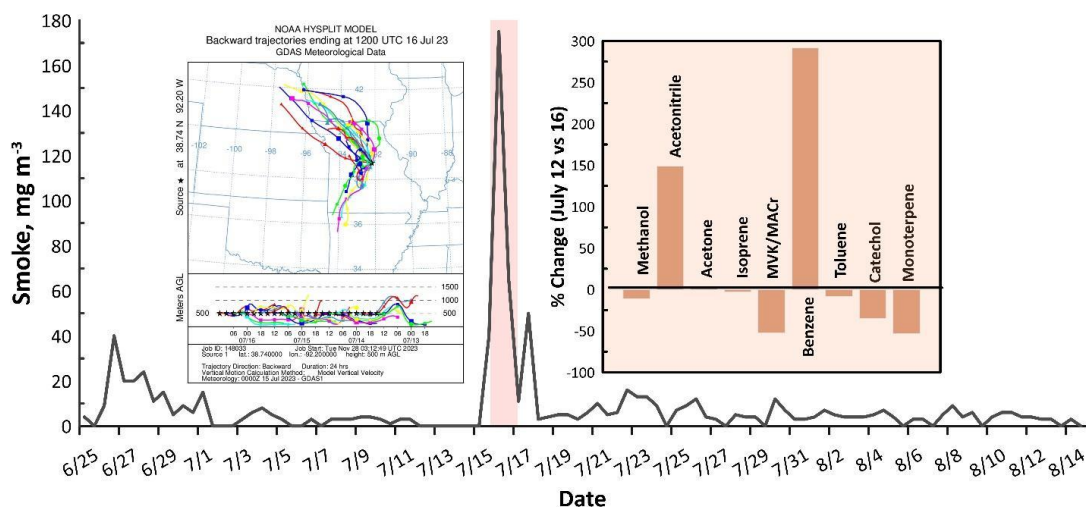
325



326 Overall, extreme temperature conditions had a mixed impact on the VOCs observed in the temperate forest. Urban
327 and combustion markers showed insensitivity to temperature variation. On the other hand, BVOCs such as isoprene,
328 MVK+MACr, and monoterpene showed linear responses but at varying rates. The alteration of VOC distribution due
329 to enhanced temperature has imminent implications on the formation of secondary aerosols, particularly under future
330 climate with expected elevated temperatures. Recent laboratory chamber studies have shown that unexpected
331 interaction of individual VOCs during the oxidation process produced intermediates and products that impacted the
332 yields, volatility, and other physiochemical properties of aerosols (Voliotis et al., 2021; Takeuchi et al., 2022; Chen
333 et al., 2022). This has a serious impact on the projection of secondary aerosol formation in the future, considering the
334 cross-reactions between intermediate products from different VOCs are not yet accounted for in secondary aerosol
335 simulations in regional and global climate models. Based on the results here, isoprene at MOFLUX is expected to
336 increase more as the temperature increases compared to monoterpene. Thus, careful consideration of the oxidant
337 chemistry and product speciation will provide valuable new insights into the impact feedback loop between aerosols
338 and climate in temperate forests.

339 **3.3 Transport of Emissions from Forest Fires**

340 In 2023, severe wildfires that were initiated by summer lightning storms occurred over several boreal forests
341 in Canada, which resulted in burning of more than 156,000 km² of cumulative area that accounted for at least 1.7% of
342 Canada's land area (Wang et al., 2023). Between May and September of 2023, carbon emissions from fires reached
343 more than 638 Tg C based on satellite observations (Byrne et al., 2023). Two air pollution episodes (June 24 to
344 July 1 and July 12 to 19) resulting from these wildfires affected the field measurement at MOFLUX. Figure 4 shows
345 the smoke concentration measured at MOFLUX. The two pollution episodes had different levels of smoke, the second
346 period having stronger enhancements compared to the first. Wildfire emissions during the first episode were
347 substantially transported to Europe, whereas the second impacted the USA to a considerable extent (Wang et al.,
348 2023). A wildfire that occurred between July 12 and 19 primarily near Fort Nelson, Northwest Canada, was transported
349 to the MOFLUX site. Back trajectory analysis (see Figure 4) indicated that the plumes arriving at the site during the
350 same period originated from the northwest, suggesting a significant long-range transport of combustion products to
351 the MOFLUX temperate forest. Atmospheric dispersion of the smoke in Missouri is presented in Figure S5.
352



353
354
355
356
357
358

Figure 4. Smoke profile observed during the field measurement. The red highlighted area is the period with intense transport of BB plumes. (Inset Left) Backward air parcel trajectory analysis of plumes arriving on the 16th of July was calculated using the Hybrid Single-Particle Lagrangian Integrated Trajectory (HYSPPLIT) Model (Stein et al., 2015). (Inset Right) Percent change of the mixing ratios of major VOCs measured during days with no combustion event (July 12) and with significant transport of BB markers (July 16).

359
360
361
362
363
364
365
366
367
368

Among the major VOCs, acetonitrile and benzene appeared to be associated with the transport of the combustion plumes. Figure 4 shows a comparison of the VOC mixing ratios during the impact of combustion plume (July 16) and non-BB event day (July 12), together with smoke mixing ratio observed at MOFLUX. These two VOCs had day average mixing ratios of 2.15 (acetonitrile) and 0.34 (benzene) ppb, corresponding to increases of 139% and 269%, respectively, compared to non-BB days. The source of benzene shifted from transport emissions to BB, highlighting the diverse anthropogenic activities impacting the variability of benzene in temperate forests. Interestingly, unsaturated BB markers like benzene can contribute to enhancement of atmospheric ozone levels (Bourgeois et al., 2021). The ozone forming potential (OFP) of benzene increased to 0.421 ppb during the transport of wildfire emissions, compared to 0.107 ppb observed on July 12, highlighting the influence of transported combustion plumes on the overall chemical reactivity in the forest (see Text S1 for the calculation of OFP).

369
370

3.4 Expanded List of VOCs and Their Response to Enhanced Temperature and Long-Range Transport of Combustion Emissions

371
372
373
374
375
376
377
378

Beyond the major VOCs discussed above, more than 250 compounds with a mass to charge ratio (m/z) of at least 40 and with mixing ratios 5 ppt above the blank measurements were identified. The proposed molecular ion formulas are listed in the Table S1. The compounds have a wide variety of molecular compositions, with 14, 23, 5, 3, and 2 maximum numbers of carbon, hydrogen, oxygen, nitrogen, and sulfur, respectively, with a median formula of C_4H_6O and a mode of 2 degrees of unsaturation. The numbers of VOCs according to atomic content were as follows: 36 C_xH_y , 93 $C_xH_yO_w$, 17 $C_xH_yN_z$, 60, $C_xH_yO_wN_z$, and 10 $C_xH_yO_wS_v$, where v , y , x , y , and z are positive integers. The median oxygen-to-carbon ratio (O:C) and hydrogen-to-carbon ratio (H:C) of all the identified ions were 0.2 and 1.4. The O:C ratio was similar to a measurement in a boreal forest in southern Finland, which can be explained by the similarity of the

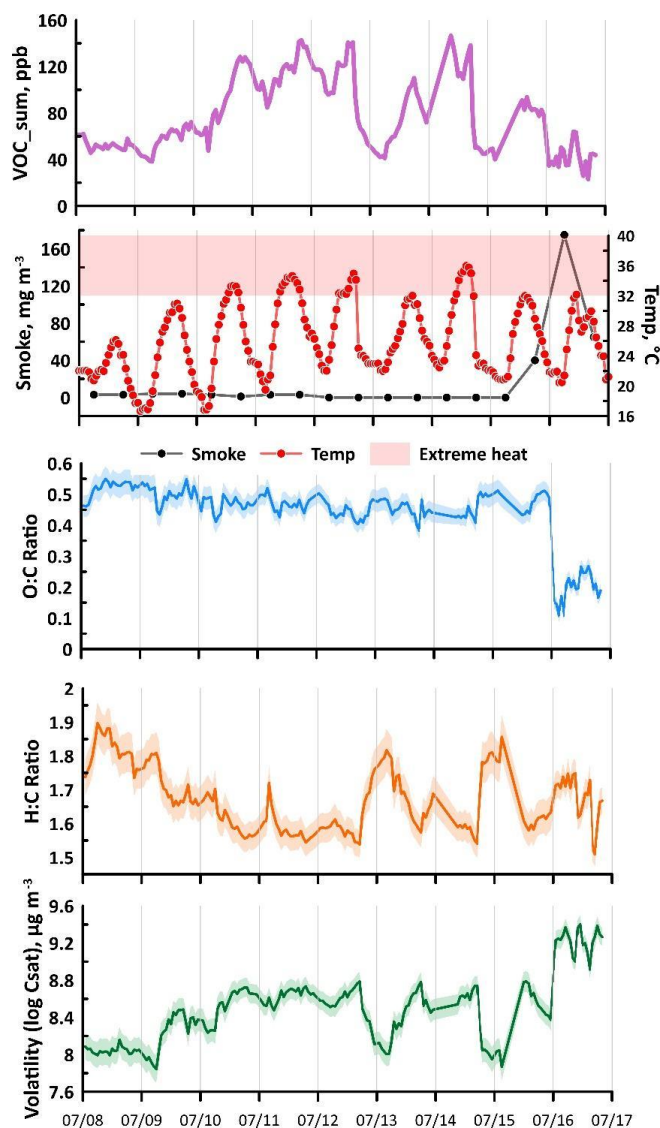


379 measurement technique applied (i.e., Vocus PTR-ToF-MS), capturing fewer oxygenated compounds compared to
380 other ionization techniques (i.e., Br and NO₃ instead of the hydronium ion) (Huang et al., 2021). The volatility of the
381 extended list of VOCs was assessed by estimating the effective saturation mass mixing ratio (C_{sat}). The
382 parameterization of the volatility, based on the number of carbon, oxygen, and nitrogen atoms (Donahue et al., 2011;
383 Mohr et al., 2019), was calculated using the following equation:

384

385
$$\log(C_{sat}) = (n_{O^*} - n_C)b_C - (n_O - 3n_N)b_O - 2\frac{(n_O - 3n_N)n_C}{(n_C + n_O - 3n_N)}b_{CO} - n_Nb_N \quad (4)$$

386 where $n_{O^*} = 25$, $b_C = 0.475$, $b_O = 0.2$, $b_{CO} = 0.9$, and $b_N = 2.5$. The terms n_C , n_O , and n_N are the number of carbon,
387 oxygen, and nitrogen atoms, respectively. The average log saturation mixing ratio for all the compounds was
388 $7.50 \mu\text{g m}^{-3}$, and 100 and 136 compounds were classified as intermediate and volatile organic compounds,
389 respectively. Log C_{sat} values below $3 \mu\text{g m}^{-3}$ were recorded for three compounds (i.e., C₆H₃NO₃, C₁₀H₁₀O₃, and
390 C₁₂H₂₃NO₃), which categorized them as semivolatile VOCs.



391

392

393

394

Figure 5. Time series profile of the sum of VOC mixing ratio, smoke, and temperature observed at MOFLUX, weighted O:C, H:C ratios, and the volatility during the intensive operational period between July 8 to 17. The shaded regions of O:C, H:C, and volatility are the weighted standard deviations.

395

396

397

398

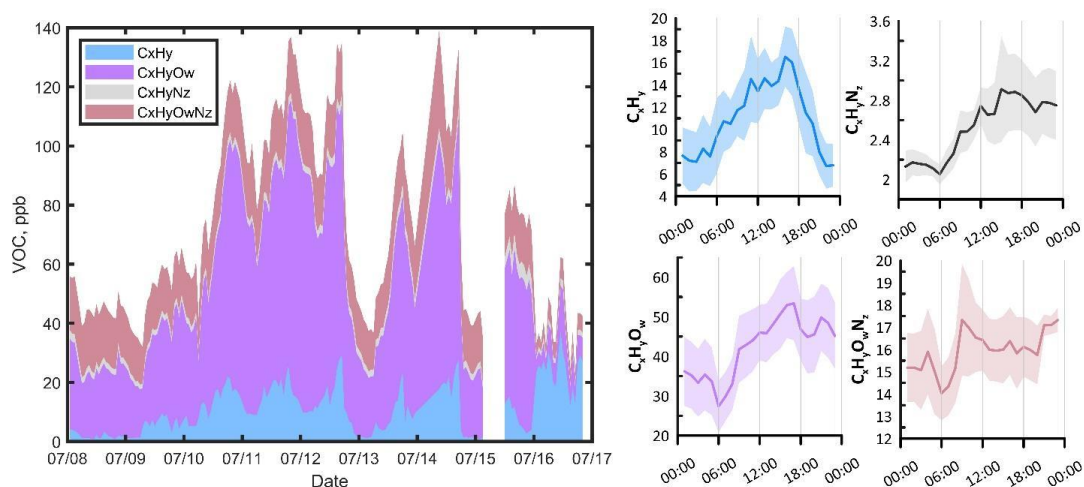
399

400

We analyzed July 8 through 17 to develop a deeper understanding of how the extended list of VOCs was influenced by extreme heat and combustion plumes. Note that in these analyses, the concentrations of acetone, isoprene, and MVK+MACr were not included to focus on the extended list of VOCs. During this period, the average VOC mixing ratio was 78 ppb. Figure 5 also shows the profile of the total VOC mixing ratios, which depicts a mixing ratio range between 23 to 147 ppb. Figure 5 illustrates the profiles of the weighted average of the O:C ratio, H:C ratio, and volatility of the VOCs. The O:C ratio was consistent, ranging between 0.4 and 0.55. However, the apparent transport



401 of the combustion plume to the site decreased the ratio to less than 0.3, indicating the dominance of the less oxygenated
 402 compounds in the atmosphere as a result of BB. The H:C ratio (1.8) was increased at the start period, characterized
 403 by low temperatures, which signifies the presence of highly unsaturated compounds such as aromatics. As the
 404 temperature increased, H:C values (1.5) decreased except during the period with biomass burning emissions (1.75),
 405 implying the alteration of VOC distribution. Lastly, elevated temperature resulted in the emission of more volatile
 406 compounds, as the weighted average volatility reached 8.5. The atmosphere over MOFLUX was further enriched with
 407 volatile compounds during the passage of the combustion plume, as the mean log C_{sat} reached $9 \mu\text{g m}^{-3}$.



408
 409 **Figure 6.** (Left) Time series and (right) diurnal profile of the clustering based on the atomic content of the VOCs during the
 410 intensive observation period with enhanced temperature and combustion plume transport at MOFLUX. $C_xH_yO_wS_v$ compounds were
 411 not included due to low mixing ratio compared to other categories.

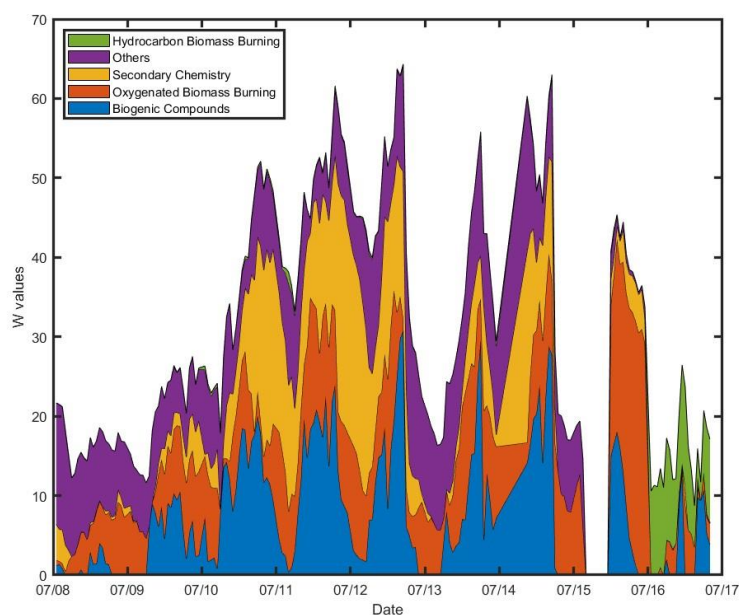
412 Figure 6 shows the profile of the extended list of VOCs, clustered according to atomic content. The decreasing order
 413 of average concentration was as follows: $C_xH_yO_w$ (41 ppb), $C_xH_yO_wN_z$ (15 ppb), C_xH_y (11 ppb), $C_xH_yN_z$ (2.4 ppb),
 414 $C_xH_yO_wS_v$ (0.48 ppb). Hydrocarbons (C_xH_y) had evident enhancement at elevated temperature, as well as during the
 415 later hours of the transport of the BB compounds on the 16th of July. Oxygenated hydrocarbons ($C_xH_yO_w$) had a
 416 delayed response to temperature, in which peak concentration occurred around 18:00. Such categories also showed
 417 increased concentration during the initial hours of combustion plume impact at MOFLUX. $C_xH_yN_z$ compounds such
 418 as acetonitrile showed clear augmentation during the initial hours of the plume transport but exhibited a less sensitive
 419 response to changes in temperature. For $C_xH_yO_wN_z$ and $C_xH_yO_wS_v$ compounds, temperature and BB had little to no
 420 effect on either group, except for the clear reduction during the latter hours of combustion plume passage in the
 421 MOFLUX temperate forest. The changes in the distribution of the extended list of VOCs, beyond the major
 422 compounds, validated the substantial influence of temperature and BB on the overall chemical reactivity of the
 423 atmosphere.

424
 425 Several compounds among the extended list showed an enhanced mixing ratio at high temperatures ($>32^\circ\text{C}$). Besides
 426 the major compounds such as isoprene and monoterpene, VOCs such as formic acid (CH_2O_2), acetic acid ($\text{C}_2\text{H}_4\text{O}_2$),



427 isocyanic acid (HCNO), acrolein (C₃H₄O), furan (C₄H₄O), methylglyoxal (C₃H₄O₂), glycolic acid (C₂H₄O₃), and
 428 propanethiol (C₃H₆S) exhibited at least 100% increases at enhanced temperature conditions. Formic and acetic acid,
 429 as two of the most dominant acids in the atmosphere, are key VOCs in aerosol growth, cloud precipitation, and
 430 rainwater acidity. Formic acid is primarily formed through photochemical production but can be emitted directly from
 431 vegetation, which is a temperature-dependent process (Millet et al., 2015). Given the anticipated increased
 432 temperatures due to extensive fossil fuel burning, addressing the enhancements of formic and acetic acid will advance
 433 our knowledge of future chemistry–climate interactions.

434 3.5 Source Apportionment of VOCs Measured during Extreme Temperature and Biomass Burning



435

436 *Figure 7. Stacked profile of the non-negative factors of species fingerprints from all the VOCs measured at MOFLUX.*

437 To systematically investigate the pattern and contributions of the extended list of VOCs, a NNMF routine was applied
 438 to study the prominent sources of the VOCs in the forest between July 8 and 17. Based on the dominant tracers,
 439 response to the range of temperatures, impact of combustion plume, and diurnal variations, five important categories
 440 were identified from the NNMF analysis: (i) Biogenic-related Compounds, (ii) Secondary Chemistry, (iii) Oxygenated
 441 BB compounds (O-BB), (iv) Hydrocarbon BB compounds (H-BB), and (v) Others. The “others” factor, with a
 442 substantial number of contributing compounds, remains unidentified.

443

444 The biogenic factor, which consisted primarily of isoprene and monoterpene, followed the profile of temperature,
 445 which supports the attribution to biogenic sources. Two BB factors were accounted for, which were separated based
 446 on the chemical composition of the gases contributing to each factor. The median formulas for O-BB and H-BB were



447 C₄H₅NO and C₆H₈, with a mode of 1 and 2 degrees of unsaturation, respectively. This is consistent with the analysis
448 based on atomic content: oxygenated hydrocarbons (C_xH_yO_w) and C_xH_yN_z compounds were persistent in the early
449 hours of the combustion plume, whereas pure hydrocarbons (C_xH_y) showed evident enhancement in the later hours of
450 July 16. Also, the saturation mixing ratio of the O-BB and H-BB factors were 7.27 and 8.45 μg m⁻³: these values place
451 both factors under the volatile category (log C_{sat} > 6 μg m⁻³). The prominent compounds under the O-BB factor were
452 acetonitrile (C₂H₃N), formamide (CH₃NO), maleic acid (C₄H₄O₂), hydroxyfuranone (C₄H₄O₃), butyramide or
453 dimethylacetamide (C₄H₉NO), benzonitrile (C₇H₅N), and furaldehyde (C₅H₅O₂), which were all previously detected
454 in field- and lab-scale measurements of combustion plumes (Jain et al., 2023; Stockwell et al., 2015; Coggon et al.,
455 2019; Salvador et al., 2022). The H-BB factor was populated by unsaturated hydrocarbons such as butadiene (C₄H₆),
456 butene (C₄H₈), pentenes (C₅H₁₀), benzene (C₆H₆), hexadiene (C₆H₁₀), and ethylbenzene (C₈H₁₀), although cyclic
457 hydrocarbons are not discounted. Interestingly, monoterpene at C₁₀H₁₇⁺ and its fragment at C₇H₈⁺ had substantial
458 contributions from the H-BB factor during this period. This is unlikely due to the expected biogenic emission in the
459 forest, although it came second with 34% contribution compared to 66% from the H-BB factor. However, several
460 prior studies have shown that monoterpene can also originate from anthropogenic activities (Coggon et al., 2021),
461 particularly BB events (Wang et al., 2022). With the enhancement of monoterpene and other unsaturated hydrocarbons
462 (e.g., butenes and ethylbenzene) during combustion plumes, several changes in atmospheric reactivity are expected,
463 such as photochemical ozone production, scavenging of OH radicals, and suppression or enhancement of aerosol
464 formation.

465

466 The secondary chemistry factor had a median chemical formula of C₃H₄O₂ with two degrees of unsaturation. Among
467 the factors identified, this factor had the highest oxygen content, with a median and max of 2 and 5, respectively.
468 Similar to the oxygenated hydrocarbon group, this factor had a diurnal profile characterized by evening enhancement
469 (~20:00). Also, the secondary factor is marked by compounds such as ethenone (C₂H₂O), acrolein (C₃H₄O), acetic
470 acid (C₂H₄O₂), MVK+MACr (C₄H₆O), hydroxyacetone (C₃H₆O₂), and acetylacetone (C₅H₈O₂). Due to its nighttime
471 peak as well as the oxidized nature of the major VOCs at this factor, it is assumed that these products are generated
472 from the nighttime oxidation using NO₃ radicals of the organics in the forest. Isoprene also generates MVK during
473 nighttime through the dominant β-RO₂ isomer formation pathway (Ng et al., 2017). During the transport of BB plumes,
474 the secondary factor had a relatively low increase in signal compared to both BB factors, which shows that oxidation
475 compounds were generally locally generated with little to no contribution from long-range transport. BB tracers
476 dominated the air mass of MOFLUX during the transport of the combustion plume, which drastically affected the
477 atmospheric chemistry of the area.

478 4. Summary and Atmospheric Implications

479 Critical VOCs, which have important contributions to several atmospheric processes, were continuously measured in
480 a temperate deciduous and juniper forest in the midwestern US during the summer of 2023 using PTR-ToF-MS.
481 During the measurement period, the forest included several sources of biogenic compounds and was influenced by
482 short- and long-range transport of anthropogenic emissions. Extreme heat and wildfire emissions impacted the



483 atmospheric conditions of the forest during the field measurement; such emissions are vital phenomena that provide
484 insights into future climate. Typical VOCs in the forest, consisting of methanol, acetone, isoprene, monoterpene,
485 MVK+MACr, benzene, toluene, acetonitrile, and catechol, had an average total mixing ratio of 69 ppb, which
486 highlights the strong effect of such VOCs on atmospheric reactivity in a temperate forest.

487

488 Among the VOCs, isoprene had one of the highest recorded mixing ratios (10 ppb), next to methanol (23 ppb) and
489 acetone (22 ppb). Enhanced temperature induced the emission of isoprene to a greater extent than did UV, based on
490 the late afternoon diurnal peak that coincides with temperature. At extreme temperature conditions, isoprene was
491 observed at twice the typical level, with a 1.32 ppb increase per 1.0°C. At the same time, for monoterpene, which was
492 suspected to be primarily ocimene or sabinene based on its daytime peak, a three-fold enhancement at extreme
493 temperatures was observed. The large gap between the mixing ratios of isoprene and monoterpene suppressed the
494 formation of aerosols due to the scavenging of OH radicals and reduction of C₂₀ dimers. AVOCs such as benzene
495 (0.42 ppb) and acetonitrile (1.52 ppb) responded much less to changes in temperature compared to the BVOCs. The
496 varying enrichment of the major VOCs and their response to extreme temperatures had a serious impact on the
497 potential aerosol formation and chemical reactivity. New studies indicated that the coexistence of multiple precursor
498 VOCs can generate unexplored molecular-scale interactions, which is critical as current and future VOC distributions
499 are expected to be widely different compared to current conditions.

500

501 Besides the role of elevated temperature, the duration of the VOC measurement at MOFLUX was marked by sporadic
502 transport of plumes from wildfires in Canada. The impending warming of the atmosphere is projected to potentially
503 increase the frequency and duration of wildfires due to drier seasons; however, increases could be significantly
504 affected regionally by accompanying changes in atmospheric circulation. In MOFLUX, the profiles of the major VOCs
505 such as benzene and acetonitrile changed notably with respect to combustion plumes, as their concentrations were
506 enhanced by more than 100%. Because benzene is an important precursor of ozone and aerosol formation, the
507 variability of such AVOCs should be included in the simulation of future atmospheric processes.

508

509 Beyond the major VOCs, analysis of the whole mass spectra revealed more than 250 other compounds, the mixing
510 ratios of which sum to as much as 78 ppb during a period with elevated temperature (>305 K) and BB plumes (smoke
511 > 100 mg m⁻³). With a similar mixing ratio sum to those of the typical VOCs, analysis of unaccounted-for VOCs is
512 necessary to perform a realistic investigation of the relevant atmospheric processes at the MOFLUX site. The O:C and
513 H:C ratios of all the VOCs, as well as their volatility, provided insight into their response to future climate scenarios.
514 During BB plume transport, less oxygenated compounds with high volatility were enhanced. Elevated temperature in
515 the forest induced the formation and emission of more unsaturated compounds. Hydrocarbons (C_xH_y) and C_xH_yN_z
516 compounds dominated the total VOC mixing ratio during the initial and later hours of biomass transport, respectively,
517 whereas oxygenated hydrocarbons persisted consistently during periods of elevated temperature. Furthermore, the
518 analysis of the entire spectra pinpointed an additional 40 compounds that have at least 100% enhancement in mixing



519 ratio at extreme temperatures. Two of them are formic (0.89 ppb) and acetic acid (3.29 ppb), which have a vital impact
520 on atmospheric acidity and cloud formation.

521

522 The highly variable profiles of the extended list of VOCs measured at MOFLUX clearly indicated that species were
523 impacted by a variety of emissions and processes. NNMF was applied to the VOC mixing ratios, and five factors were
524 identified: two BB factors and one each for secondary chemistry, biogenic, and others. The two BB factors were
525 resolved based on the chemical composition of the compounds contributing to each factor. With the high reactivity of
526 such compounds to oxidants such as OH and NO₃, it is expected that BB altered the normal forest-dominated
527 atmospheric processes.

528

529 The comprehensive analysis of the whole mass spectra performed in this study underscores the importance of
530 unaccounted-for VOCs in the total chemical reactivity of the atmosphere. The results of this study highlight the
531 possible unaccounted modifications in VOC distribution that might be expected in future climate scenarios with
532 serious impacts on aerosol–climate interaction. With the growing but still limited insights on the effect of mixed
533 precursors on aerosol formation, more information regarding the overall distribution and transformation of AVOCs
534 and BVOCs and their response to different future climate scenarios are needed to realistically account for the climate
535 forcing of organic aerosols.

536



537 **Data availability**

538 The data used in this publication are available to the community and can be accessed by request to the corresponding
539 author.

540 **Author contribution:**

541 CMS, JDW, EGC, HAS, BDK, and SSO conducted the measurements. CMS, JDW, MAM, KRB, and GL designed
542 the project, coordinated the measurements, and supervised the study. MAM, GL, and KRB obtained funding for the
543 project. CMS and KRB carried out the data curation and analysis. CMS prepared the manuscript. All co-authors
544 contributed to the discussion and the interpretation of the results.

545 **Competing interests:**

546 The authors declare that they have no conflict of interest.

547 **Acknowledgements**

548 This research was funded through Oak Ridge National Laboratory (ORNL)'s Directed Research and Development
549 (LDRD) program. ORNL is managed by the University of Tennessee-Battelle, LLC, under contract DE-AC05-
550 00OR22725 with the U.S. Department of Energy. The U.S. Drought Monitor, which provided the drought data of
551 Boone County, MO, is jointly produced by the National Drought Mitigation Center at the University of Nebraska-
552 Lincoln, the United States Department of Agriculture, and the National Oceanic and Atmospheric Administration.
553 The authors gratefully acknowledge the NOAA Air Resources Laboratory (ARL) for the provision of the HYSPLIT
554 transport and dispersion model (<https://www.ready.noaa.gov>) used in this publication.

555

556

Reference

557

- 558 Ambrose, J. L., Haase, K., Russo, R. S., Zhou, Y., White, M. L., Frinak, E. K., Jordan, C., Mayne, H. R., Talbot, R.,
559 and Sive, B. C.: A comparison of GC-FID and PTR-MS toluene measurements in ambient air under conditions
560 of enhanced monoterpene loading, *Atmos. Meas. Tech.*, 3, 959-980, 10.5194/amt-3-959-2010, 2010.
- 561 Bates, K. H., Jacob, D. J., Wang, S., Hornbrook, R. S., Apel, E. C., Kim, M. J., Millet, D. B., Wells, K. C., Chen, X.,
562 Brewer, J. F., Ray, E. A., Commane, R., Diskin, G. S., and Wofsy, S. C.: The Global Budget of Atmospheric
563 Methanol: New Constraints on Secondary, Oceanic, and Terrestrial Sources, *J. Geophys. Res. Atmos.*, 126,
564 e2020JD033439, <https://doi.org/10.1029/2020JD033439>, 2021.
- 565 Blake, R. S., Monks, P. S., and Ellis, A. M.: Proton-Transfer Reaction Mass Spectrometry, *Chem. Rev.*, 109, 861-
566 896, 10.1021/cr800364q, 2009.
- 567 Borsdorf, H., Bentele, M., Müller, M., Rebmann, C., and Mayer, T.: Comparison of Seasonal and Diurnal
568 Concentration Profiles of BVOCs in Coniferous and Deciduous Forests, *Atmosphere*, 14, 1347, 2023.
- 569 Bourgeois, I., Peischl, J., Neuman, J. A., Brown, S. S., Thompson, C. R., Aikin, K. C., Allen, H. M., Angot, H.,
570 Apel, E. C., Baublitz, C. B., Brewer, J. F., Campuzano-Jost, P., Commane, R., Crouse, J. D., Daube, B. C.,
571 DiGangi, J. P., Diskin, G. S., Emmons, L. K., Fiore, A. M., Gkatzelis, G. I., Hills, A., Hornbrook, R. S., Huey,
572 L. G., Jimenez, J. L., Kim, M., Lacey, F., McKain, K., Murray, L. T., Nault, B. A., Parrish, D. D., Ray, E.,
573 Sweeney, C., Tanner, D., Wofsy, S. C., and Ryerson, T. B.: Large contribution of biomass burning emissions to



- 574 ozone throughout the global remote troposphere, *Proc. Natl. Acad. Sci.*, 118, e2109628118,
575 doi:10.1073/pnas.2109628118, 2021.
- 576 Byrne, B., Liu, J., Bowman, K., Pascolini-Campbell, M., Chatterjee, A., Pandey, S., Miyazaki, K., van der Werf, G.,
577 Wunch, D., and Wennberg, P.: Unprecedented Canadian forest fire carbon emissions during 2023, 2023.
- 578 Chen, T., Zhang, P., Chu, B., Ma, Q., Ge, Y., Liu, J., and He, H.: Secondary organic aerosol formation from mixed
579 volatile organic compounds: Effect of RO₂ chemistry and precursor concentration, *npj Climate and*
580 *Atmospheric Science*, 5, 95, 10.1038/s41612-022-00321-y, 2022.
- 581 Coggon, M. M., Lim, C. Y., Koss, A. R., Sekimoto, K., Yuan, B., Gilman, J. B., Hagan, D. H., Selimovic, V.,
582 Zarzana, K. J., Brown, S. S., Roberts, J. M., Müller, M., Yokelson, R., Wisthaler, A., Krechmer, J. E., Jimenez,
583 J. L., Cappa, C., Kroll, J. H., de Gouw, J., and Warneke, C.: OH chemistry of non-methane organic gases
584 (NMOGs) emitted from laboratory and ambient biomass burning smoke: evaluating the influence of furans and
585 oxygenated aromatics on ozone and secondary NMOG formation, *Atmos. Chem. Phys.*, 19, 14875-14899,
586 10.5194/acp-19-14875-2019, 2019.
- 587 Coggon, M. M., Gkatzelis, G. I., McDonald, B. C., Gilman, J. B., Schwantes, R. H., Abuhassan, N., Aikin, K. C.,
588 Arend, M. F., Berkoff, T. A., Brown, S. S., Campos, T. L., Dickerson, R. R., Gronoff, G., Hurley, J. F.,
589 Isaacman-VanWertz, G., Koss, A. R., Li, M., McKeen, S. A., Moshary, F., Peischl, J., Pospisilova, V., Ren, X.,
590 Wilson, A., Wu, Y., Trainer, M., and Warneke, C.: Volatile chemical product emissions enhance ozone and
591 modulate urban chemistry, *Proc. Natl. Acad. Sci.*, 118, e2026653118, doi:10.1073/pnas.2026653118, 2021.
- 592 Collins, M., Knutti, R., Arblaster, J., Dufresne, J.-L., Fichetef, T., Friedlingstein, P., Gao, X., Gutowski, W. J.,
593 Johns, T., and Krinner, G.: Long-term climate change: projections, commitments and irreversibility, 2013.
- 594 Daussy, J. and Staudt, M.: Do future climate conditions change volatile organic compound emissions from
595 *Artemisia annua*? Elevated CO₂ and temperature modulate actual VOC emission rate but not its emission
596 capacity, *Atmospheric Environment: X*, 7, 100082, <https://doi.org/10.1016/j.aeoa.2020.100082>, 2020.
- 597 Donahue, N. M., Epstein, S. A., Pandis, S. N., and Robinson, A. L.: A two-dimensional volatility basis set: 1.
598 organic-aerosol mixing thermodynamics, *Atmos. Chem. Phys.*, 11, 3303-3318, 10.5194/acp-11-3303-2011,
599 2011.
- 600 Ferracci, V., Bolas, C. G., Freshwater, R. A., Staniaszek, Z., King, T., Jaars, K., Otu-Larbi, F., Beale, J., Malhi, Y.,
601 Waine, T. W., Jones, R. L., Ashworth, K., and Harris, N. R. P.: Continuous Isoprene Measurements in a UK
602 Temperate Forest for a Whole Growing Season: Effects of Drought Stress During the 2018 Heatwave,
603 *Geophysical Research Letters*, 47, e2020GL088885, <https://doi.org/10.1029/2020GL088885>, 2020.
- 604 Finewax, Z., de Gouw, J. A., and Ziemann, P. J.: Identification and Quantification of 4-Nitrocatechol Formed from
605 OH and NO₃ Radical-Initiated Reactions of Catechol in Air in the Presence of NO_x: Implications for Secondary
606 Organic Aerosol Formation from Biomass Burning, *Environ. Sci. Technol.*, 52, 1981-1989,
607 10.1021/acs.est.7b05864, 2018.
- 608 Fuentes, J. D. and Wang, D.: ON THE SEASONALITY OF ISOPRENE EMISSIONS FROM A MIXED
609 TEMPERATE FOREST, *Ecological Applications*, 9, 1118-1131, [https://doi.org/10.1890/1051-0761\(1999\)009\[1118:OTSOIE\]2.0.CO;2](https://doi.org/10.1890/1051-0761(1999)009[1118:OTSOIE]2.0.CO;2), 1999.



- 611 Gentner, D. R., Ormeño, E., Fares, S., Ford, T. B., Weber, R., Park, J. H., Brioude, J., Angevine, W. M., Karlik, J.
612 F., and Goldstein, A. H.: Emissions of terpenoids, benzenoids, and other biogenic gas-phase organic compounds
613 from agricultural crops and their potential implications for air quality, *Atmos. Chem. Phys.*, 14, 5393-5413,
614 10.5194/acp-14-5393-2014, 2014.
- 615 Geron, C., Daly, R., Harley, P., Rasmussen, R., Seco, R., Guenther, A., Karl, T., and Gu, L.: Large drought-induced
616 variations in oak leaf volatile organic compound emissions during PINOT NOIR 2012, *Chemosphere*, 146, 8-
617 21, <https://doi.org/10.1016/j.chemosphere.2015.11.086>, 2016.
- 618 Greenberg, J. P., Guenther, A. B., Pétron, G., Wiedinmyer, C., Vega, O., Gatti, L. V., Tota, J., and Fisch, G.:
619 Biogenic VOC emissions from forested Amazonian landscapes, *Global Change Biology*, 10, 651-662,
620 <https://doi.org/10.1111/j.1365-2486.2004.00758.x>, 2004.
- 621 Gu, L., Pallardy, S. G., Hosman, K. P., and Sun, Y.: Drought-influenced mortality of tree species with different
622 predawn leaf water dynamics in a decade-long study of a central US forest, *Biogeosciences*, 12, 2831-2845,
623 10.5194/bg-12-2831-2015, 2015.
- 624 Guenther, A. B., Jiang, X., Heald, C. L., Sakulyanontvittaya, T., Duhl, T., Emmons, L. K., and Wang, X.: The
625 Model of Emissions of Gases and Aerosols from Nature version 2.1 (MEGAN2.1): an extended and updated
626 framework for modeling biogenic emissions, *Geosci. Model Dev.*, 5, 1471-1492, 10.5194/gmd-5-1471-2012,
627 2012.
- 628 Hakola, H., Hellén, H., Hemmilä, M., Rinne, J., and Kulmala, M.: In situ measurements of volatile organic
629 compounds in a boreal forest, *Atmos. Chem. Phys.*, 12, 11665-11678, 10.5194/acp-12-11665-2012, 2012.
- 630 Hallquist, M., Wenger, J. C., Baltensperger, U., Rudich, Y., Simpson, D., Claeys, M., Dommen, J., Donahue, N. M.,
631 George, C., Goldstein, a. H., Hamilton, J. F., Herrmann, H., Hoffmann, T., Iinuma, Y., Jang, M., Jenkin, M. E.,
632 Jimenez, J. L., Kiendler-Scharr, a., Maenhaut, W., McFiggans, G., Mentel, T. F., Monod, a., Prévôt, a. S. H.,
633 Seinfeld, J. H., Surratt, J. D., Szmigielski, R., and Wildt, J.: The formation, properties and impact of secondary
634 organic aerosol: current and emerging issues, *Atmos. Chem. Phys.*, 9, 5155-5236, 10.5194/acp-9-5155-2009,
635 2009.
- 636 Heinritzi, M., Dada, L., Simon, M., Stolzenburg, D., Wagner, A. C., Fischer, L., Ahonen, L. R., Amanatidis, S.,
637 Baalbaki, R., Baccarini, A., Bauer, P. S., Baumgartner, B., Bianchi, F., Brilke, S., Chen, D., Chiu, R., Dias, A.,
638 Dommen, J., Duplissy, J., Finkenzeller, H., Frege, C., Fuchs, C., Garmash, O., Gordon, H., Granzin, M., El
639 Haddad, I., He, X., Helm, J., Hofbauer, V., Hoyle, C. R., Kangasluoma, J., Keber, T., Kim, C., Kürten, A.,
640 Lamkaddam, H., Laurila, T. M., Lampilahti, J., Lee, C. P., Lehtipalo, K., Leiminger, M., Mai, H., Makhmutov,
641 V., Manninen, H. E., Marten, R., Mathot, S., Mauldin, R. L., Mentler, B., Molteni, U., Müller, T., Nie, W.,
642 Nieminen, T., Onnela, A., Partoll, E., Passananti, M., Petäjä, T., Pfeifer, J., Pospisilova, V., Quéléver, L. L. J.,
643 Rissanen, M. P., Rose, C., Schobesberger, S., Scholz, W., Scholze, K., Sipilä, M., Steiner, G., Stozhkov, Y.,
644 Tauber, C., Tham, Y. J., Vazquez-Pufleau, M., Virtanen, A., Vogel, A. L., Volkamer, R., Wagner, R., Wang,
645 M., Weitz, L., Wimmer, D., Xiao, M., Yan, C., Ye, P., Zha, Q., Zhou, X., Amorim, A., Baltensperger, U.,
646 Hansel, A., Kulmala, M., Tomé, A., Winkler, P. M., Worsnop, D. R., Donahue, N. M., Kirkby, J., and Curtius,



- 647 J.: Molecular understanding of the suppression of new-particle formation by isoprene, *Atmos. Chem. Phys.*, 20,
648 11809-11821, 10.5194/acp-20-11809-2020, 2020.
- 649 Hu, L., Millet, D. B., Kim, S. Y., Wells, K. C., Griffis, T. J., Fischer, E. V., Helmig, D., Hueber, J., and Curtis, A. J.:
650 North American acetone sources determined from tall tower measurements and inverse modeling, *Atmos.*
651 *Chem. Phys.*, 13, 3379-3392, 10.5194/acp-13-3379-2013, 2013.
- 652 Huang, W., Li, H., Sarnela, N., Heikkinen, L., Tham, Y. J., Mikkilä, J., Thomas, S. J., Donahue, N. M., Kulmala,
653 M., and Bianchi, F.: Measurement report: Molecular composition and volatility of gaseous organic compounds
654 in a boreal forest – from volatile organic compounds to highly oxygenated organic molecules, *Atmos. Chem.*
655 *Phys.*, 21, 8961-8977, 10.5194/acp-21-8961-2021, 2021.
- 656 Huangfu, Y., Yuan, B., Wang, S., Wu, C., He, X., Qi, J., de Gouw, J., Warneke, C., Gilman, J. B., Wisthaler, A.,
657 Karl, T., Graus, M., Jobson, B. T., and Shao, M.: Revisiting Acetonitrile as Tracer of Biomass Burning in
658 Anthropogenic-Influenced Environments, *Geophysical Research Letters*, 48, e2020GL092322,
659 <https://doi.org/10.1029/2020GL092322>, 2021.
- 660 Jain, V., Tripathi, N., Tripathi, S. N., Gupta, M., Sahu, L. K., Murari, V., Gaddamidi, S., Shukla, A. K., and Prevot,
661 A. S. H.: Real-time measurements of non-methane volatile organic compounds in the central Indo-Gangetic
662 basin, Lucknow, India: source characterisation and their role in O₃ and secondary organic aerosol formation,
663 *Atmos. Chem. Phys.*, 23, 3383-3408, 10.5194/acp-23-3383-2023, 2023.
- 664 Jardine, K. J., Jardine, A. B., Holm, J. A., Lombardozi, D. L., Negron-Juarez, R. I., Martin, S. T., Beller, H. R.,
665 Gimenez, B. O., Higuchi, N., and Chambers, J. Q.: Monoterpene ‘thermometer’ of tropical forest-atmosphere
666 response to climate warming, *Plant, Cell & Environment*, 40, 441-452, <https://doi.org/10.1111/pce.12879>, 2017.
- 667 Jardine, K. J., Chambers, J. Q., Holm, J., Jardine, A. B., Fontes, C. G., Zorzanelli, R. F., Meyers, K. T., De Souza,
668 V. F., Garcia, S., Gimenez, B. O., Piva, L. R. d. O., Higuchi, N., Artaxo, P., Martin, S., and Manzi, A. O.: Green
669 Leaf Volatile Emissions during High Temperature and Drought Stress in a Central Amazon Rainforest, *Plants*,
670 4, 678-690, 2015.
- 671 Kanawade, V. P., Jobson, B. T., Guenther, A. B., Erupe, M. E., Pressley, S. N., Tripathi, S. N., and Lee, S. H.:
672 Isoprene suppression of new particle formation in a mixed deciduous forest, *Atmos. Chem. Phys.*, 11, 6013-
673 6027, 10.5194/acp-11-6013-2011, 2011.
- 674 Kiendler-Scharr, A., Wildt, J., Maso, M. D., Hohaus, T., Kleist, E., Mentel, T. F., Tillmann, R., Uerlings, R., Schurr,
675 U., and Wahner, A.: New particle formation in forests inhibited by isoprene emissions, *Nature*, 461, 381-384,
676 http://www.nature.com/nature/journal/v461/n7262/supinfo/nature08292_S1.html, 2009.
- 677 Lantz, A. T., Allman, J., Weraduwege, S. M., and Sharkey, T. D.: Control of rate and physiological role of isoprene
678 emission from plants, *Plant, cell & environment*, 42, 2808, 2019a.
- 679 Lantz, A. T., Solomon, C., Gog, L., McClain, A. M., Weraduwege, S. M., Cruz, J. A., and Sharkey, T. D.: Isoprene
680 Suppression by CO₂ Is Not Due to Triose Phosphate Utilization (TPU) Limitation, *Frontiers in Forests and*
681 *Global Change*, 2, 10.3389/ffgc.2019.00008, 2019b.
- 682 Lee, J.-Y., Marotzke, J., Bala, G., Cao, L., Corti, S., Dunne, J. P., Engelbrecht, F., Fischer, E., Fyfe, J. C., and Jones,
683 C.: Future global climate: scenario-based projections and near-term information, in: *Climate change 2021: The*



684 physical science basis. Contribution of working group I to the sixth assessment report of the intergovernmental
685 panel on climate change, Cambridge University Press, 553-672, 2021.

686 Lee, S.-H., Uin, J., Guenther, A. B., de Gouw, J. A., Yu, F., Nadykto, A. B., Herb, J., Ng, N. L., Koss, A., Brune, W.
687 H., Baumann, K., Kanawade, V. P., Keutsch, F. N., Nenes, A., Olsen, K., Goldstein, A., and Ouyang, Q.:
688 Isoprene suppression of new particle formation: Potential mechanisms and implications, *J. Geophys. Res.*
689 *Atmos.*, 121, 14,621-614,635, <https://doi.org/10.1002/2016JD024844>, 2016.

690 Li, L., Tang, P., Nakao, S., Chen, C. L., and Cocker Iii, D. R.: Role of methyl group number on SOA formation
691 from monocyclic aromatic hydrocarbons photooxidation under low-NOx conditions, *Atmos. Chem. Phys.*, 16,
692 2255-2272, 10.5194/acp-16-2255-2016, 2016.

693 Ling, Z., He, Z., Wang, Z., Shao, M., and Wang, X.: Sources of methacrolein and methyl vinyl ketone and their
694 contributions to methylglyoxal and formaldehyde at a receptor site in Pearl River Delta, *Journal of*
695 *Environmental Sciences*, 79, 1-10, <https://doi.org/10.1016/j.jes.2018.12.001>, 2019.

696 McFiggans, G., Mentel, T. F., Wildt, J., Pullinen, I., Kang, S., Kleist, E., Schmitt, S., Springer, M., Tillmann, R.,
697 Wu, C., Zhao, D., Hallquist, M., Faxon, C., Le Breton, M., Hallquist, Å. M., Simpson, D., Bergström, R.,
698 Jenkin, M. E., Ehn, M., Thornton, J. A., Alfarra, M. R., Bannan, T. J., Percival, C. J., Priestley, M., Topping,
699 D., and Kiendler-Scharr, A.: Secondary organic aerosol reduced by mixture of atmospheric vapours, *Nature*,
700 565, 587-593, 10.1038/s41586-018-0871-y, 2019.

701 Millet, D. B., Baasandorj, M., Farmer, D. K., Thornton, J. A., Baumann, K., Brophy, P., Chaliyakunnel, S., de
702 Gouw, J. A., Graus, M., Hu, L., Koss, A., Lee, B. H., Lopez-Hilfiker, F. D., Neuman, J. A., Paulot, F., Peischl,
703 J., Pollack, I. B., Ryerson, T. B., Warneke, C., Williams, B. J., and Xu, J.: A large and ubiquitous source of
704 atmospheric formic acid, *Atmos. Chem. Phys.*, 15, 6283-6304, 10.5194/acp-15-6283-2015, 2015.

705 Mohr, C., Thornton, J. A., Heitto, A., Lopez-Hilfiker, F. D., Lutz, A., Riipinen, I., Hong, J., Donahue, N. M.,
706 Hallquist, M., Petäjä, T., Kulmala, M., and Yli-Juuti, T.: Molecular identification of organic vapors driving
707 atmospheric nanoparticle growth, *Nature Communications*, 10, 4442, 10.1038/s41467-019-12473-2, 2019.

708 Montzka, S. A., Trainer, M., Angevine, W. M., and Fehsenfeld, F. C.: Measurements of 3-methyl furan, methyl
709 vinyl ketone, and methacrolein at a rural forested site in the southeastern United States, *J. Geophys. Res.*
710 *Atmos.*, 100, 11393-11401, <https://doi.org/10.1029/95JD01132>, 1995.

711 Navarro, M. A., Dusanter, S., and Stevens, P. S.: Temperature dependence of the yields of methacrolein and methyl
712 vinyl ketone from the OH-initiated oxidation of isoprene under NOx-free conditions, *Atmos. Environ.*, 79, 59-
713 66, <https://doi.org/10.1016/j.atmosenv.2013.06.032>, 2013.

714 Ng, N. L., Kroll, J. H., Chan, A. W. H., Chhabra, P. S., Flagan, R. C., and Seinfeld, J. H.: Secondary organic aerosol
715 formation from *m*-xylene, toluene, and benzene, *Atmos. Chem. Phys.*, 7, 3909-3922, 10.5194/acp-7-
716 3909-2007, 2007.

717 Ng, N. L., Brown, S. S., Archibald, A. T., Atlas, E., Cohen, R. C., Crowley, J. N., Day, D. A., Donahue, N. M., Fry,
718 J. L., Fuchs, H., Griffin, R. J., Guzman, M. I., Herrmann, H., Hodzic, A., Iinuma, Y., Jimenez, J. L., Kiendler-
719 Scharr, A., Lee, B. H., Luecken, D. J., Mao, J., McLaren, R., Mutzel, A., Osthoff, H. D., Ouyang, B., Picquet-
720 Varrault, B., Platt, U., Pye, H. O. T., Rudich, Y., Schwantes, R. H., Shiraiwa, M., Stutz, J., Thornton, J. A.,



- 721 Tilgner, A., Williams, B. J., and Zaveri, R. A.: Nitrate radicals and biogenic volatile organic compounds:
722 oxidation, mechanisms, and organic aerosol, *Atmos. Chem. Phys.*, 17, 2103-2162, 10.5194/acp-17-2103-2017,
723 2017.
- 724 Park, S., Allen, R. J., and Lim, C. H.: A likely increase in fine particulate matter and premature mortality under
725 future climate change, *Air Quality, Atmosphere & Health*, 13, 143-151, 10.1007/s11869-019-00785-7, 2020.
- 726 Patiny, L. and Borel, A.: ChemCalc: A Building Block for Tomorrow's Chemical Infrastructure, *Journal of*
727 *Chemical Information and Modeling*, 53, 1223-1228, 10.1021/ci300563h, 2013.
- 728 Potosnak, M. J., LeStourgeon, L., Pallardy, S. G., Hosman, K. P., Gu, L., Karl, T., Geron, C., and Guenther, A. B.:
729 Observed and modeled ecosystem isoprene fluxes from an oak-dominated temperate forest and the influence of
730 drought stress, *Atmos. Environ.*, 84, 314-322, <https://doi.org/10.1016/j.atmosenv.2013.11.055>, 2014.
- 731 Ramasamy, S., Ida, A., Jones, C., Kato, S., Tsurumaru, H., Kishimoto, I., Kawasaki, S., Sadanaga, Y., Nakashima,
732 Y., Nakayama, T., Matsumi, Y., Mochida, M., Kagami, S., Deng, Y., Ogawa, S., Kawana, K., and Kajii, Y.:
733 Total OH reactivity measurement in a BVOC dominated temperate forest during a summer campaign, 2014,
734 *Atmos. Environ.*, 131, 41-54, <https://doi.org/10.1016/j.atmosenv.2016.01.039>, 2016.
- 735 Ruffault, J., Curt, T., Martin-StPaul, N. K., Moron, V., and Trigo, R. M.: Extreme wildfire events are linked to
736 global-change-type droughts in the northern Mediterranean, *Nat. Hazards Earth Syst. Sci.*, 18, 847-856,
737 10.5194/nhess-18-847-2018, 2018.
- 738 Safronov, A. N., Shtabkin, Y. A., Berezina, E. V., Skorokhod, A. I., Rakitin, V. S., Belikov, I. B., and Elansky, N.
739 F.: Isoprene, Methyl Vinyl Ketone and Methacrolein from TROICA-12 Measurements and WRF-CHEM and
740 GEOS-CHEM Simulations in the Far East Region, *Atmosphere*, 10, 152, 2019.
- 741 Sahu, A., Mostofa, M. G., Weraduwege, S. M., and Sharkey, T. D.: Hydroxymethylbutenyl diphosphate
742 accumulation reveals MEP pathway regulation for high CO₂-induced suppression of isoprene
743 emission, *Proc. Natl. Acad. Sci.*, 120, e2309536120, doi:10.1073/pnas.2309536120, 2023.
- 744 Salvador, C. M., Chou, C. C. K., Ho, T. T., Tsai, C. Y., Tsao, T. M., and Su, T. C.: Contribution of Terpenes to
745 Ozone Formation and Secondary Organic Aerosols in a Subtropical Forest Impacted by Urban Pollution,
746 *Atmosphere*, 11, 1232, 2020a.
- 747 Salvador, C. M., Chou, C. C. K., Cheung, H. C., Ho, T. T., Tsai, C. Y., Tsao, T. M., Tsai, M. J., and Su, T. C.:
748 Measurements of submicron organonitrate particles: Implications for the impacts of NO_x pollution in a
749 subtropical forest, *Atmospheric Research*, 245, 105080, <https://doi.org/10.1016/j.atmosres.2020.105080>, 2020b.
- 750 Salvador, C. M., Chou, C. C. K., Ho, T. T., Ku, I. T., Tsai, C. Y., Tsao, T. M., Tsai, M. J., and Su, T. C.: Extensive
751 urban air pollution footprint evidenced by submicron organic aerosols molecular composition, *npj Climate and*
752 *Atmospheric Science*, 5, 96, 10.1038/s41612-022-00314-x, 2022.
- 753 Salvador, C. M. C., C. -K.; Ho, T.-T.; Tsai, C.-Y.; Tsao, T.-M.; Tsai, M.-J.; Su, T.-C.: Contribution of Terpenes to
754 Ozone Formation and Secondary Organic Aerosols in a Subtropical Forest Impacted by Urban Pollution,
755 *Atmosphere*, 11, 1232, 2020.



- 756 Sarris, D., Christopoulou, A., Angelonidi, E., Koutsias, N., Fulé, P. Z., and Arianoutsou, M.: Increasing extremes of
757 heat and drought associated with recent severe wildfires in southern Greece, *Regional Environmental Change*,
758 14, 1257-1268, 10.1007/s10113-013-0568-6, 2014.
- 759 Schneider, E., Czech, H., Popovicheva, O., Chichaeva, M., Kobelev, V., Kasimov, N., Minkina, T., Rüger, C. P.,
760 and Zimmermann, R.: Mass spectrometric analysis of unprecedented high levels of carbonaceous aerosol
761 particles long-range transported from wildfires in the Siberian Arctic, *Atmos. Chem. Phys.*, 24, 553-576,
762 10.5194/acp-24-553-2024, 2024a.
- 763 Schneider, S. R., Shi, B., and Abbatt, J. P. D.: The Measured Impact of Wildfires on Ozone in Western Canada from
764 2001 to 2019, *J. Geophys. Res. Atmos.*, 129, e2023JD038866, <https://doi.org/10.1029/2023JD038866>, 2024b.
- 765 Seco, R., Karl, T., Guenther, A., Hosman, K. P., Pallardy, S. G., Gu, L., Geron, C., Harley, P., and Kim, S.:
766 Ecosystem-scale volatile organic compound fluxes during an extreme drought in a broadleaf temperate forest of
767 the Missouri Ozarks (central USA), *Global Change Biology*, 21, 3657-3674, <https://doi.org/10.1111/gcb.12980>,
768 2015.
- 769 Shen, L., Mickley, L. J., and Murray, L. T.: Influence of 2000–2050 climate change on particulate matter in the
770 United States: results from a new statistical model, *Atmos. Chem. Phys.*, 17, 4355-4367, 10.5194/acp-17-4355-
771 2017, 2017.
- 772 Shtabkin, Y. A., Safronov, A. N., Berezina, E. V., and Skorokhod, A. I.: The comparison between the isoprene,
773 methyl vinyl ketone and methacrolein concentrations measured in the TROICA-12 expedition at Far East
774 region, *IOP Conference Series: Earth and Environmental Science*, 231, 012047, 10.1088/1755-
775 1315/231/1/012047, 2019.
- 776 Spirig, C., Guenther, A., Greenberg, J. P., Calanca, P., and Tarvainen, V.: Tethered balloon measurements of
777 biogenic volatile organic compounds at a Boreal forest site, *Atmos. Chem. Phys.*, 4, 215-229, 10.5194/acp-4-
778 215-2004, 2004.
- 779 Stein, A., Draxler, R. R., Rolph, G. D., Stunder, B. J., Cohen, M., and Ngan, F.: NOAA’s HYSPLIT atmospheric
780 transport and dispersion modeling system, *Bulletin of the American Meteorological Society*, 96, 2059-2077,
781 2015.
- 782 Stewart, G. J., Nelson, B. S., Drysdale, W. S., Acton, W. J. F., Vaughan, A. R., Hopkins, J. R., Dunmore, R. E.,
783 Hewitt, C. N., Nemitz, E., Mullinger, N., Langford, B., Shivani, Reyes-Villegas, E., Gadi, R., Rickard, A. R.,
784 Lee, J. D., and Hamilton, J. F.: Sources of non-methane hydrocarbons in surface air in Delhi, India, *Faraday*
785 *Discuss.*, 226, 409-431, 10.1039/D0FD00087F, 2021.
- 786 Stockwell, C. E., Veres, P. R., Williams, J., and Yokelson, R. J.: Characterization of biomass burning emissions
787 from cooking fires, peat, crop residue, and other fuels with high-resolution proton-transfer-reaction time-of-
788 flight mass spectrometry, *Atmospheric Chemistry and Physics*, 15, 845-865, 10.5194/acp-15-845-2015, 2015.
- 789 Takeuchi, M., Berkemeier, T., Eris, G., and Ng, N. L.: Non-linear effects of secondary organic aerosol formation
790 and properties in multi-precursor systems, *Nature Communications*, 13, 7883, 10.1038/s41467-022-35546-1,
791 2022.



- 792 Varga, K., Jones, C., Trugman, A., Carvalho, L. M. V., McLoughlin, N., Seto, D., Thompson, C., and Daum, K.:
793 Megafires in a Warming World: What Wildfire Risk Factors Led to California's Largest Recorded Wildfire,
794 *Fire*, 5, 16, 2022.
- 795 Vermeuel, M. P., Novak, G. A., Kilgour, D. B., Claflin, M. S., Lerner, B. M., Trowbridge, A. M., Thom, J., Cleary,
796 P. A., Desai, A. R., and Bertram, T. H.: Observations of biogenic volatile organic compounds over a mixed
797 temperate forest during the summer to autumn transition, *Atmos. Chem. Phys.*, 23, 4123-4148, 10.5194/acp-23-
798 4123-2023, 2023.
- 799 Voliotis, A., Wang, Y., Shao, Y., Du, M., Bannan, T. J., Percival, C. J., Pandis, S. N., Alfarra, M. R., and
800 McFiggans, G.: Exploring the composition and volatility of secondary organic aerosols in mixed anthropogenic
801 and biogenic precursor systems, *Atmos. Chem. Phys.*, 21, 14251-14273, 10.5194/acp-21-14251-2021, 2021.
- 802 Wang, H., Ma, X., Tan, Z., Wang, H., Chen, X., Chen, S., Gao, Y., Liu, Y., Liu, Y., Yang, X., Yuan, B., Zeng, L.,
803 Huang, C., Lu, K., and Zhang, Y.: Anthropogenic monoterpenes aggravating ozone pollution, *National Science*
804 *Review*, 9, 10.1093/nsr/nwac103, 2022.
- 805 Wang, Z., Wang, Z., Zou, Z., Chen, X., Wu, H., Wang, W., Su, H., Li, F., Xu, W., Liu, Z., and Zhu, J.: Severe
806 Global Environmental Issues Caused by Canada's Record-Breaking Wildfires in 2023, *Advances in*
807 *Atmospheric Sciences*, 10.1007/s00376-023-3241-0, 2023.
- 808 Wells, K. C., Millet, D. B., Cady-Pereira, K. E., Shephard, M. W., Henze, D. K., Bousserez, N., Apel, E. C., de
809 Gouw, J., Warneke, C., and Singh, H. B.: Quantifying global terrestrial methanol emissions using observations
810 from the TES satellite sensor, *Atmos. Chem. Phys.*, 14, 2555-2570, 10.5194/acp-14-2555-2014, 2014.
- 811 Wennberg, P. O., Bates, K. H., Crounse, J. D., Dodson, L. G., McVay, R. C., Mertens, L. A., Nguyen, T. B., Praske,
812 E., Schwantes, R. H., and Smarte, M. D.: Gas-phase reactions of isoprene and its major oxidation products,
813 *Chem. Rev.*, 118, 3337-3390, 2018.
- 814 Wiedinmyer, C., Tie, X., Guenther, A., Neilson, R., and Granier, C.: Future Changes in Biogenic Isoprene
815 Emissions: How Might They Affect Regional and Global Atmospheric Chemistry?, *Earth Interactions*, 10, 1-19,
816 <https://doi.org/10.1175/EI174.1>, 2006.
- 817 Wiedinmyer, C., Greenberg, J., Guenther, A., Hopkins, B., Baker, K., Geron, C., Palmer, P. I., Long, B. P., Turner,
818 J. R., Pétron, G., Harley, P., Pierce, T. E., Lamb, B., Westberg, H., Baugh, W., Koerber, M., and Janssen, M.:
819 Ozarks Isoprene Experiment (OZIE): Measurements and modeling of the "isoprene volcano", *J. Geophys. Res.*
820 *Atmos.*, 110, <https://doi.org/10.1029/2005JD005800>, 2005.
- 821 Yu, H., Ortega, J., Smith, J. N., Guenther, A. B., Kanawade, V. P., You, Y., Liu, Y., Hosman, K., Karl, T., Seco, R.,
822 Geron, C., Pallardy, S. G., Gu, L., Mikkilä, J., and Lee, S.-H.: New Particle Formation and Growth in an
823 Isoprene-Dominated Ozark Forest: From Sub-5 nm to CCN-Active Sizes, *Aerosol Science and Technology*, 48,
824 1285-1298, 10.1080/02786826.2014.984801, 2014.
- 825 Yuan, B., Koss, A. R., Warneke, C., Coggon, M., Sekimoto, K., and de Gouw, J. A.: Proton-Transfer-Reaction Mass
826 Spectrometry: Applications in Atmospheric Sciences, *Chem. Rev.*, 117, 13187-13229,
827 10.1021/acs.chemrev.7b00325, 2017.
- 828